

IS THE HIGH- z LYNX ARC NEBULA IONIZED BY AN OBSCURED QSO?

L. Binette,¹ B. Groves,² M. Villar-Martín,³ R. A. E. Fosbury,⁴ and D. J. Axon⁵

RESUMEN

El arco gravitacional observado por Holden en el año 2001 a $z = 3.356$ presenta fuertes líneas de emisión como C IV $\lambda\lambda 1549$, O III] $\lambda 1665$ pero no N V $\lambda 1240$. Se considera la posibilidad de que la fuente ionizante sea una ley de potencia (AGN) parcialmente absorbida. Comparamos las razones de las líneas de una nebulosa de baja metalicidad ($Z_{\text{total}} = 0.05Z_{\odot}$) fotoionizada por una fuente como la propuesta con aquellas producidas por una estrella de metalicidad cero y una $T_{\text{eff}} = 80\,000$ K. Bien usando un continuo térmico o bien un AGN absorbido, todos los modelos dan como resultado líneas de [O II] $\lambda\lambda 3727$ muy débiles.

ABSTRACT

The gravitational arc observed by Holden in 2001 at $z = 3.356$ reveals strong emission lines of N IV] $\lambda 1485$, C IV $\lambda\lambda 1549$, O III] $\lambda 1665$ but no N V $\lambda 1240$. We consider the possibility that the ionizing source consisting of a partially absorbed powerlaw. We compare the line ratios from a low metallicity nebula ($Z_{\text{total}} = 0.05Z_{\odot}$) photoionized by such filtered continuum with those produced by a zero-metallicity star of $T_{\text{eff}} = 80\,000$ K. Whether using a thermal or an absorbed AGN continuum, all models result in very weak [O II] $\lambda\lambda 3727$ lines.

Key Words: **COSMOLOGY: MISCELLANEOUS — LINE: FORMATION — QUASARS: EMISSION LINES**

1. INTRODUCTION

The Lynx arc, with a redshift of 3.357, was discovered during spectroscopic follow-up (Holden, Stanford & Rosati 2001; hereafter HN01) of the $z = 0.570$ cluster RX J0848+4456 from the ROSAT Deep Cluster Survey. The arc is characterized by a very red R-K color and strong, narrow emission lines, whose ratios are unusual. In this contribution, we consider the possibility that a modified AGN continuum might account for the main features of the Lynx arc nebula. More details on the method used and the justification for the different ionizing spectral energy distributions (ISED) presented here were given in Binette, Groves, Villar-Martín, Fosbury & Axon (2003; hereafter BGVFA). While we do not argue here that the Lynx arc spectrum necessarily requires ionization by an AGN, we believe it is important to show that such an explanation has a degree of diagnostic plausibility. Fosbury, Villar-Martín, Humphrey et al. (2003) presented an alternative interpretation consisting of photoionization by a metal poor stellar cluster. In their discovery paper of the Lynx arc, HN01 had proposed a blackbody ISED.

2. PHOTOIONIZATION CALCULATIONS

2.1. The stellar energy distribution

As thermal distribution and for comparison purposes, we used a stellar ISED of $T_{\text{eff}} = 80\,000$ K derived from the work of Schaerer (2002), which in terms of the proportion of He⁺ ionizing photons is equivalent to a blackbody of 67 200 K (a temperature in accord with the suggestion of HN01). The resulting stellar energy distribution is plotted in Fig. 1 (long-dashed line).

2.2. A partly absorbed powerlaw

The alternative excitation mechanism studied in this contribution consists of photoionization by a partly absorbed AGN powerlaw. Dense layers of gas near the central engine and hidden from our view would be responsible for modifying significantly the intrinsic powerlaw from the active nucleus. The misalignment of the emerging ionizing cone relative to our line-of-sight would explain why this putative screen and the quasar are hidden from our view (as a result of a dusty and opaque torus around the black hole). The emission lines that are observed would originate from low density *extranuclear narrow line region* gas (hereafter ENLR) photoionized by the emerging filtered powerlaw. The geometry that we envisage, except for the presence here of an absorption filter, is analogous to that of the detached nebulosity in Pks2152–69 in which the separation between the bright ENLR cloud and the parent AGN

¹Instituto de Astronomía, UNAM, México.

²Mt. Stromlo Observatory, Australia.

³Instituto de Astrofísica de Andalucía, Spain.

⁴ST-ECF, Germany.

⁵Dept. of Physics, Rochester Inst. of Tech., NY, USA.

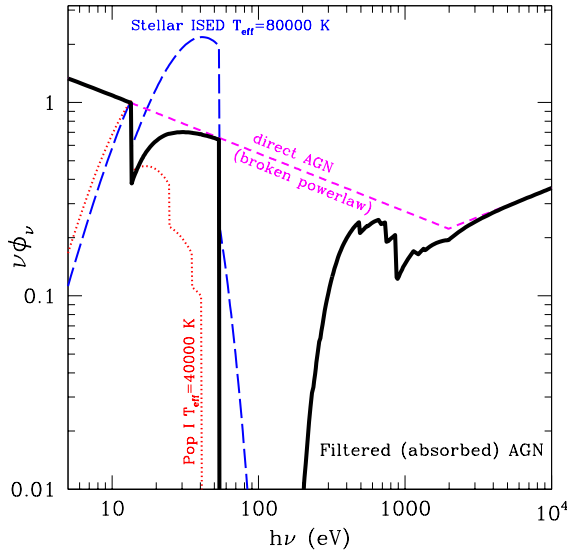


Fig. 1. Spectral energy distributions in $\nu\phi_\nu$ of the four input ionizing distributions used in the photoionization calculations presented in Table 1. These are: the direct AGN broken powerlaw (short-dashed line), the emerging filtered distribution (thick line), the zero-metallicity 80 000 K stellar atmosphere (long-dashed line) and the 40 000 K POP I stellar atmosphere (dotted line). The scale is arbitrary. The filtered distribution still contains 80% of the number of ionizing photons originally present in the direct broken powerlaw (Sect. 2.2).

is of order 8 kpc (Tadhunter, Fosbury, di Serego Alighieri et al. 1988).

Specifically, we will assume that the filtering gas layers absorb radiation at the very high ionization parameter, $U_{\text{fil}} = 2$, is very dense, $n_{\text{H}}^{\text{fil}} \sim 10^{11} \text{ cm}^{-3}$, and has the same total metallicity as the (visible) ENLR (i.e. 5% solar).

We have set the He^+ opacity of the filter to be such that the narrow line nebular $\text{He II}/\text{H}\beta$ ratio calculated using the *absorbed* AGN continuum as input (in photoionization calculations of the ENLR) becomes comparable to that produced by the stellar ISED shown above. With $U_{\text{fil}} = 2$, this occurs when the filtering layer *absorbs* $\simeq 20\%$ of Q_{H} , the ionizing photon luminosity (by photon number). The intrinsic energy distribution assumed for the central engine (before the filter) is a broken powerlaw, as in Binette, Wilson, Raga & Storchi-Bergmann (1997). The ISED emerging from the putative filter and later reprocessed into emission lines by the ENLR nebula is plotted in Fig. 1 (thick line).

2.3. The gas phase abundances and dust

In order to reveal the main differences between nebulae photoionized by an absorbed powerlaw con-

tinuum and a $\sim 80\,000$ K stellar atmosphere, it is imperative to use the same nebular parameters: dust content, gas metallicity, gas density and ionization parameter. For the ionization parameter, we simply adopt the value favored by HN01 of $U_{\text{neb}} = 0.1$ and for the total (dust + gas) nebular abundances Z_{total} , we adopt their suggested metallicity of 5% solar. For helium, we assumed the primordial value of $\text{He}/\text{H} = 0.075$. We adopted a gas density of $n_{\text{H}}^{\text{neb}} = 10^3 \text{ cm}^{-3}$ and a simple slab geometry. Our models include internal dust, at a level of 2.5% of that of the solar neighborhood value, which is half of the expected value if the dust content scaled linearly with Z_{total} .

3. MODEL RESULTS AND DISCUSSION

The photoionization calculations using the the 80 000 K stellar distribution and the absorbed (broken) powerlaw distribution are presented in columns 3 and 4 of Table 1, respectively. For comparison purposes, we present in columns 5 and 7, respectively, photoionization calculations using the *direct* (broken) powerlaw distribution and a 40 000 K POP I stellar distribution (Hummer & Mihalas 1970). These ISED are plotted in Fig. 1. Note that the absorbed continuum presents a very large He^+ absorption trough between 54.4 eV and 300 eV, much deeper than that caused by H^0 between 13.6 and ~ 30 eV. This deeper trough obviously accounts for the somewhat weaker He II lines (Col. 4) of the absorbed case as compared to the direct powerlaw (Col. 5).

3.1. Comparison of the nebular structure

The very low gas metallicity is the basic explanation for the high nebular temperatures of models. This favors generating unusually strong collisionally excited UV lines which are characterized by larger excitation energies than optical lines. One important reason why the 80 000 K star ISED is so remarkably efficient in generating strong high excitation UV lines is that the bulk of its ionizing photons lie within the narrow energy band 20–54.4 eV, which is crucial in maintaining a relatively large fraction of ions in the triply ionized stage, a condition facilitating the reproduction of the strong C IV and $\text{N IV}]$ lines of the Lynx arc.

3.2. Line ratios and ISED comparisons

Inspection of Table 1 shows that the absorbed powerlaw and the 80 000 K atmosphere produce line ratios which are often comparable. For instance, comparison of Cols. 3 and 4 shows that although

TABLE 1
LINE RATIOS FROM PHOTOIONIZATION CALCULATIONS^{a,b}

| Line ID | λ (\AA) | Hot star 80 000 K | AGN Absorbed ^c | AGN Direct | AGN Absorbed ^c | Pop I 40 000 K |
|--|-------------------------------|----------------------|------------------------------|---------------|------------------------------|-------------------|
| (1) | (2) | (3) | (4) | (5) | (6) | (7) |
| | Z_{gas}/Z_{\odot} : | 0.038 | 0.038 | 0.038 | $3 \times 0.038^{\text{d}}$ | 0.038 |
| H β | 4861 | 1.00 | 1.00 | 1.00 | 1.00 | 1.00 |
| He II | 1640 | 0.095 | 0.13 | 1.24 | 0.14 | <0.001 |
| He II | 4686 | 0.011 | 0.015 | 0.14 | 0.018 | <0.001 |
| C II] | 2326 | 0.003 | 0.034 | 0.026 | 0.098 | 0.008 |
| C III] | 1909 | 0.96 | 0.785 | 0.47 | 1.44 | 1.47 |
| C IV | 1549 | 3.28 | 1.60 | 0.82 | 2.77 | 0.002 |
| N III] | 1749 | 0.040 | 0.055 | 0.047 | 0.10 | 0.172 |
| N IV] | 1485 | 0.32 | 0.25 | 0.17 | 0.40 | <0.001 |
| N v | 1240 | < 0.001 | 0.098 | 0.20 | 0.17 | <0.001 |
| [O I] | 6300 | 0.001 | 0.29 | 0.24 | 0.75 | <0.001 |
| [O II] | 3727 | 0.02 | 0.09 | 0.078 | 0.27 | 0.08 |
| [O III] | 5007 | 6.07 | 4.68 | 2.98 | 11.6 | 4.72 |
| O III] | 1665 | 0.79 | 0.95 | 0.58 | 1.55 | 0.36 |
| O VI | 1035 | <0.001 | 0.16 | 1.41 | 0.26 | <0.001 |
| [S II] | 6731 | 0.002 | 0.25 | 0.20 | 0.63 | <0.001 |
| S IV] | 1406 | 0.015 | 0.022 | 0.012 | 0.028 | 0.006 |
| Mg II | 2800 | 0.016 | 0.11 | 0.084 | 0.32 | 0.013 |
| Si III] | 1887 | 0.0015 | 0.0023 | 0.0022 | 0.0051 | 0.03 |
| Si IV | 1397 | 0.018 | 0.022 | 0.015 | 0.043 | 0.135 |
| [Ne III] | 3869 | 0.65 | 0.51 | 0.29 | 1.21 | 0.39 |
| [Ne v] | 3426 | < 0.001 | 0.043 | 0.134 | 0.088 | <0.001 |
| $\langle T(\text{H}^+) \rangle$ | (K) | 21900 | 25700 | 33000 | 21200 | 18100 |
| $\langle T(\text{C}^{+3}) \rangle$ | (K) | 22300 | 23700 | 24300 | 19900 | 18200 |
| $\langle \text{C}^{+2}/\text{C} \rangle$ | – | 0.363 | 0.287 | 0.192 | 0.286 | 0.988 |
| $\langle \text{C}^{+3}/\text{C} \rangle$ | – | 0.628 | 0.207 | 0.099 | 0.223 | – |
| $\langle \text{C}^{+4}/\text{C} \rangle$ | – | 0.005 | 0.242 | 0.273 | 0.246 | – |
| $h(\nu - \nu_0)_{\nu \geq \nu_0}^{\nu < 4\nu_0}$ | (eV) | 15.2 | 12.6 | 10.4 | 12.6 | 6.4 |

^aAll line ratios are expressed relative to H β .

^bAll models assume $U_{\text{neb}} = 0.1$, a density $n_{\text{H}}^{\text{neb}} = 10^3 \text{ cm}^{-3}$ (See Sect. 2.3) and an ionization-bounded slab geometry with the ionized fraction of H not exceeding 1% at the back of the slab.

^cUsing the *filtered* AGN ionizing energy distribution plotted in Fig. 1 (thick solid line).

^dModel with three times higher gas phase metallicity but same dust content.

the C IV is twice as weak in the case of the absorbed ISED, the other strong lines like C III], N III], N IV], He II and O III] λ 1665 in the UV and [Ne III] and [O III] λ 5007 in the optical, differ by less than 50% between the two models.

Having shown that the strongest UV lines detected in the Lynx arc nebula (N IV], C IV, O III] and He II) can be accounted for, in principle, by a filtered

AGN continuum, we now review which differences stand up between an absorbed continuum and the 80 000 K stellar ISED.

Inspection of Table 1 shows that the UV lines of N v λ 1240, O VI λ 1035, [Ne v] λ 3426, Mg II λ 2800 and C II] λ 2326, although weak and somewhat difficult to detect, would be good discriminants, since they are so much brighter in the filtered AGN case

as compared to the stellar case. In the optical, we find that the [O I] and [S II] lines are much stronger in the absorbed case while their detection would cause a problem to the stellar interpretation. However, such lines are intrinsically weak and, furthermore, their strength is critically dependent on whether or not the nebula is fully thick to the Lyman radiation. In the absorbed ISED case, the systematic larger strengths of all the low ionization lines result obviously from the strong soft X-ray component (0.4–1.5 keV) which is responsible for creating a large *partially ionized zone*.

Interestingly, the ratio [O II]/[O III] is unusually small in all models. This results essentially from the very high ionization parameter employed. The largest ratio (0.035) is produced by the absorbed powerlaw. It is dubious whether such a small ratio could be measure in very high redshift objects.

While the UV spectrum is clearly unusual in the Lynx arc nebula, the optical spectrum as far as the [O III] or [Ne III] lines are concerned is not unusual. It is tempting to conclude that whenever [O II] is absent in a high redshift nebulae or when its spectrum is characterized by a very low [O II]/[O III] upper limit, it is possible that such nebulae might share more similarities with the Lynx nebula than with normal albeit luminous H II regions.

4. CONCLUSIONS

The absorbed powerlaw distribution *can* reproduce qualitatively the line-spectrum observed in the Lynx arc nebula. It also predicts (rest-frame) optical

lines of [O I] and [S II] and UV lines of Mg II and C II which are substantial stronger than in the hot stellar ISED case. Furthermore, any detection of even weak N V λ 1240, O VI λ 1035 or [Ne V] λ 3426 would clearly favor the absorbed AGN continuum interpretation. Independently of the question of which ISED is the most appropriate, the absence of the [O II] λ 3727 lines in high redshift nebulae optical spectra may be indicator of physical conditions not unlike those of the Lynx arc.

The work of LB was supported by the CONA-CyT grant F-40096 and that of BG by the Alex Rodgers Traveling Fellowship, the Astronomical Society of Australia as well as the RSAA. RAEF is affiliated to the Space Telescopes Division of the Research and Space Science Department, the European Space Agency.

REFERENCES

- Binette, L., Wilson, A. S., Raga, A. & Storchi-Bergmann, T. 1997, A&A, 327, 909
 Binette, L., Groves, B., Villar-Martín, M., Fosbury, R. A. E. & Axon, D. J. 2003, A&A, 405, 975 (BGVFA)
 Fosbury, R. A. E., Villar-Martín, M., Humphrey, A., Lombardi, M., et al. 2003, ApJ, 596, 797
 Holden, B. P., Stanford, S. A., Rosati, P., et al. 2001, AJ, 122, 629 (HN01)
 Hummer, D. G., & Mihalas, D. 1970, MNRAS, 147, 339
 Schaerer, D. 2002, A&A, 382, 28
 Tadhunter, C. N., Fosbury, R. A. E., di Serego Alighieri, S., Bland, J., et al. 1988, MNRAS, 235, 403

- L. Binette: Instituto de Astronomía, UNAM, Ap. 70-264, 04510 D. F., México (binette@astroscu.unam.mx).
 B. Groves: Mt. Stromlo Observatory, Cotter Rd., Weston Creek, ACT 2611 (bgroves@mso.anu.edu.au).
 M. Villar-Martín: Instituto de Astrofísica de Andalucía, Apdo. 3004, 18080 Granada, Spain (montse@iaa.es).
 R. A. E. Fosbury: ST-ECF, Karl Schwarzschild Str. 2, 85748 Garching-bei-München, Germany (rfosbury@eso.org).
 D. J. Axon: Dept. of Physics, Rochester Institute of Technology, 85 Lomb Memorial Dr., Rochester, NY 14623-5603, USA (djasps@osfmail.isc.rit.edu).